Improving the Triple Coupled Ring-Resonator Performance as an Optical Filter

Fatemeh Bazouband[a,*] and Amin Rahimpour[b]

[a]Department of Physics, Faculty of Science, Fasa University, Fasa, Iran
[b]Electronic Engineering, Faculty of Engineering, Islamic Azad University of Fasa Branch, Fasa, Iran

*Corresponding author email: fbazooband@gmail.com

ABSTRACT— In this paper, a three ring-resonator serially coupled is considered as an optical filter. We are going to improve the performance of the designed optical filter by increasing the quality factor and finesse of filtered wavelengths. The first and last rings are coupled to the bus waveguides that carry the input and output fields. The effect of coupling parameters and ring radii on the filtering of operating wavelengths which are between 1545-1550 *nm* with narrow Free Spectral Range (FSR) less than 0.5 nm is investigated. Using the transfer matrix method, all the rotating and output fields are obtained. FSR, Full Width at Half Maximum (FWHM) and Finesse (F) are evaluated by the wavelength response plots of the output ports obtained in Wolfram Mathematica. The behavior of structure is analyzed by a new approach in order to filter the resonant wavelengths of the transmission channel with higher finesse.

KEYWORDS: coupled ring-resonators, optical filter, coupling coefficients, radius of ring.

I. INTRODUCTION

Optical ring resonators have been used as very useful tools in the optical integrated circuits since many years ago [1]–[39]. They do not require bulky electrical cavities and complex optical structures for the light feedback. So, they can be made in small micrometer configurations and different combinations of them have been used for many applications [3], [4], [6], [11], [13], [16], [18], [21]–[28], [31], [32], [38]–[40]. Sequence of ring resonators have been widely used as optical filters [3], [4], [10], [13], [16], [21]–[23], [25], [26], [28], [29], [37]. Diverse structures have been explored, among which the Coupled Resonator Optical Waveguide (CROW) as shown in Fig. 1, is one of the most applied [11]–[13], [15], [16], [20], [26], [32]. The structure is investigated in this paper with a different approach as an optical filter. The first decade of the history of CROWs was discussed in the article review [12] from the original idea to the latest applications. Since then, there have been many studies in the CROWs, which are discussed below.
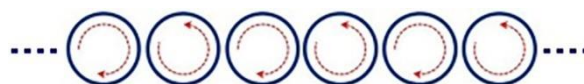

Fig. 1. Schematic view of a coupled-resonator optical waveguide (CROW), dotted red lines show the propagation direction of fields in the ring resonators.

CROW-based band-pass filter in TriPleX™ technology was proposed experimentally for microwave photonic signal processing [13]. A full-wave finite difference time domain study of ideal and disordered CROW was presented in [11]. A novel optical single-sideband modulation system by employing an optical band-pass filter based on silicon-on-insulator CROWs demonstrated experimentally in [26]. Quantum and thermal noise limits of CROW was analyzed theoretically [32]. High order exceptional points of degeneracy was generated in [41] by a novel theoretical approach in photonic structures based on CROWs. A review

and perspective of CROWs as optical delay lines was presented in [18].

In this paper, the CROW with three micro-rings is considered as an optical filter. The filtering performance of the desired structure is improved by investigating the effect of coupling coefficients and ring radii on the filtering of resonant wavelengths with higher finesse. Up to our knowledge, we haven't seen this approach for affecting the performance of CROW as an optical filter. The system is analyzed in Sec. II by the coupled mode theory and transfer matrix technique [3], [6], [15], [20], [32], [41]. Numerical results are shown in Sec. III and the concluding remarks are made in Sec. IV.

II. THEORETICAL MODEL

The structure described in this paper as shown in Fig. 2, consists of three serially coupled rings which coupled at the beginning and end to two bus waveguides. The input fields $\left(E_{in}, E_{add}\right)$ that are continuous waves enter from the input channels and after guiding through the rings, specified frequencies according to the resonant frequency of structure, are filtered or passed from the output ports. In Fig. 2, the output ports carry output fields E_{tr}, E_{dr}, called transmission and dropping channel respectively. In the designed structure of CROW it is possible to change the resonant frequencies of the structure by changing the coupling coefficients or the radius of rings. Because the optical path-length varies and resonant wavelengths that occur when the optical length is multiple of wavelength, will be affected. Also, the coupling between the rings causes the variation of full width at half maximum intensity of resonant frequencies. Therefore, it is possible to narrow or widen the filtered bands depending on the application.

By considering the lossless coupling region $\left(\chi_j^2 + r_j^2 = 1\right)$ and formulating this area [33], the relations of the fields, as shown in Fig. 2, are as following:

$$E_{a,j+1} = i\chi_j \exp\left(\frac{i\kappa L_{j+1} - \alpha L_{j+1}}{2}\right) E_{a,j} +$$
$$+ r_j \exp\left(\frac{i\kappa L_{j+1} - \alpha L_{j+1}}{2}\right) E_{b,j+1},$$

(1a)

$$E_{b,j} = r_j E_{a,j} + i\chi_j \exp\left(\frac{i\kappa L_{j+1} - \alpha L_{j+1}}{2}\right) E_{b,j+1},$$

(1b)

where α is the loss coefficient, L_j is the circumference of jth ring and χ_j and r_j and r_j are the coupling and transmission coefficient of jth ring to $(j+1)^{th}$ ring respectively. The wavelength of propagating mode is λ with the wavenumber $\kappa = 2n\pi/\lambda$ and n is the refractive index of the ring material. According to this denomination, the coupling parameters of the first ring to bus waveguide are χ_0 and r_0 By solving two relations of Eq. (1) with two variables $E_{a,j+1}, E_{b,j+1}$, the transfer matrix of coupling region is given as,

$$M_j = \begin{pmatrix} \dfrac{i}{\chi_j}\exp\left(\dfrac{i\kappa - \alpha}{2}L_{j+1}\right) & \dfrac{-ir_j}{\chi_j}\exp\left(\dfrac{i\kappa - \alpha}{2}L_{j+1}\right) \\ \dfrac{ir_j}{\chi_j}\exp\left(-\dfrac{i\kappa - \alpha}{2}L_{j+1}\right) & \dfrac{-i}{\chi_j}\exp\left(-\dfrac{i\kappa - \alpha}{2}L_{j+1}\right) \end{pmatrix}.$$
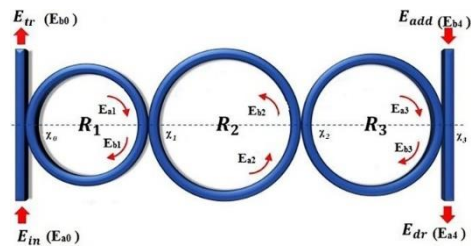
(2)

Fig. 2. Three serially coupled rings (CROW with three rings) and the propagating electric fields. R_j is the ring radius, χ_j is the coupling coefficients where j=0-3.

To find the output fields, this matrix is multiplied by itself N times, where N is the number of coupling regions. For the last ring, it should be noted that the phase statement in the last matrix will be zero $\left(L_4 = 0\right)$. If $T = \sum\limits_{j=1}^{4} M_j$

denotes the total transfer matrix of the structure, assuming no signal is received from the second waveguide $(E_{b,4} = 0.0)$, the ratio of the output-to-input fields according to the components of this matrix is obtained as following:

$$\begin{bmatrix} E_{a,4} \\ 0 \end{bmatrix} = \mathbf{T} \begin{bmatrix} E_{a,0} \\ E_{b,0} \end{bmatrix},$$

$$\frac{E_{drop}}{E_{in}} = \frac{E_{a,4}}{E_{a,0}} = \frac{T_{11} \times T_{22} - T_{12} \times T_{21}}{T_{22}}, \qquad (3)$$

$$\frac{E_{through}}{E_{in}} = \frac{E_{b,0}}{E_{a,0}} = \frac{-T_{21}}{T_{22}}.$$

By the mentioned matrix method, all field intensities of the structure can be calculated and analyzed. The corresponding math operations and drawing of the diagrams were performed using Mathematica software.

III. ANALYTICAL RESULTS

Cascade ring resonators are more prominent than single ring resonator due to their ability to vary the frequency spectrum [3], [6], [7], [18], [19], [25]. Because of the coupling regions between the rings in cascade ring resonators, the field is transferred through the rings and the optical path-length varies. When light of the resonant wavelength is passed through the rings, it builds up in intensity over multiple round-trips due to constructive interference. Therefore, the resonant frequencies that filter or pass in different output channels and cause maximum or minimum intensity vary and the frequency spectrum is affected.

CROW is one of the most famous cascade ring resonators. In this study, CROW with three rings is considered to investigate the effect of coupling coefficients and ring radii on the filtering with higher finesse and quality factor [34]. A quality measure of the microring is the Finesse F, which is the ratio between the FSR and FWHM $(F = FSR/FWHM)$. A parameter which is closely related to the finesse is the quality factor Q of a resonator, which is a measure of the sharpness of the resonance and is defined as the ratio of the operating wavelength and the resonance width $(Q = \lambda/FWHM)$. FSR is defined as the difference in position between two consecutive resonant peaks and FWHM is the width of a resonance for a specific wavelength.

Adding rings to this structure increases greatly the effective parameters on the desired purpose which leads to the confusion of the investigation. However, decreasing the number of rings, increases the FWHM as shown in Fig. 4 and causes the lower quality factor. Therefore, three coupled rings are considered in this paper for the better understanding of the effect of the desired parameters on the efficient filtering. The ring resonators and coupling regions are considered lossless and the silicon-on-insulator ring [39] with the refractive index $n=3.45$ is applied. A typical silicon-on-insulator (SOI) wafer consists a thin layer of single-crystalline silicon (Si) separated from the bulk silicon substrate by a layer of silicon oxide (SiO$_2$). The fabrication process of SOI microring devices, like what is theoretically analyzed in this study, was discussed completely in chapter 4 of [42]. SOI coupled ring resonators made up of small silicon blocks with high refractive index $n_2=3.45$ are surrounded by a silicon oxide SiO$_2$ bottom cladding ($n=1.4$) and a low index top cladding (air), as shown in Fig. 3 for desired number of rings. The presence of a material with high refractive index (the waveguide core) surrounded by a material with lower refractive index leads to total internal reflection phenomena that forces the beam to bounce back inside the core each time it reaches the waveguide walls.
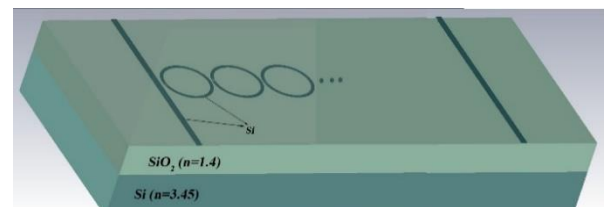

Fig. 3. Schematic view, not at scale, of a CROW waveguide fabricated on SOI chip.

Many studies have been done to investigate how changing the bending radii, waveguide coupling lengths or coupling gaps affects the

coupling area and leads to specific coupling coefficients [42]–[52]. According to the reported experimental results the applied coupling coefficients in the present study are achievable in practice for the used geometric properties of the structure.

Transmission channel spectrum of CROW with three rings is compared in Fig. 4 with that of single ring. I_T and I_{In} are the field intensity of transmission and input channels, respectively. For the simplicity, all of the coupling coefficients and ring radii are considered the same $(\chi = 0.7, R = 80 \mu m)$. It is seen that the coupling between the rings cause changing the resonance modes and so, more wavelengths are filtered relative to the single ring. Also, the quality factor of the structure is increased about 30% comparing to the single ring, because of decreasing the FWHM.
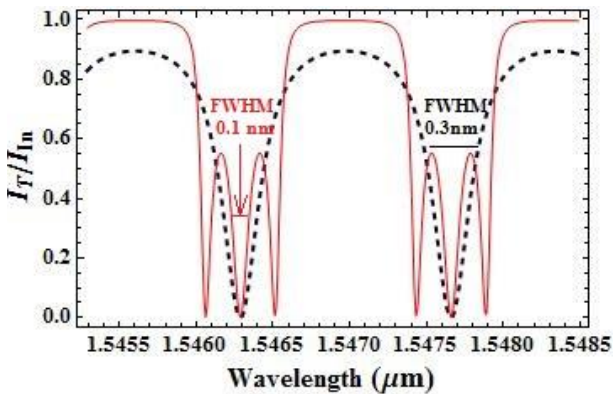

Fig. 4. Comparison of transmission channel spectrum of CROW with three rings (solid-line) and CROW with single ring (dashed-line). I_T and I_{In} are the field intensity of transmission and input channels, respectively $(\chi = 0.7, R = 80 \mu m)$.

In the CROW structure with three rings, the parameters affecting the performance of the system are so much and it is very difficult to find the optimal filtering in the transmission channel. Hence, first, we investigate the effect of several different ring radii while all the coupling coefficients are the same, then, by choosing the best radii, the effect of coupling coefficients on the filter improvement is investigated. In Fig. 5, the transmission spectrum is shown for the CROW with the same ring radii while all the coupling coefficients are $\chi = 0.7$ and three conditions are compared. In

blue solid-line, ring radii are $R = 20 \mu m$, in red solid-line: $R = 80 \mu m$ and in black dashed-line: $R = 150 \mu m$. As shown in the figure, although increasing the radius of rings causes filtering of more wavelengths at the specified range with smaller FWHM, infinitely large radii cannot be selected to filter more signals. Since, by increasing the radius, the FSR is also decreased, so, the finesse is not improved.
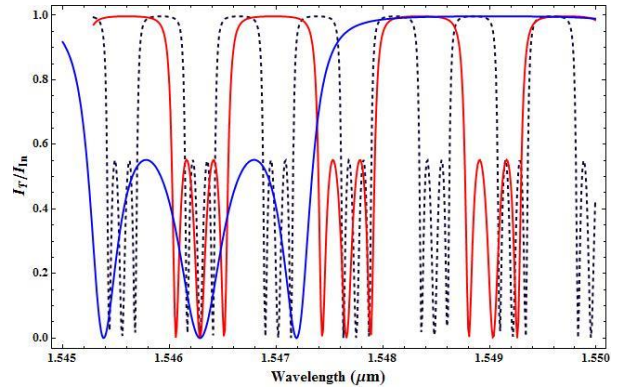

Fig. 5. The transmission spectrum of CROW with three rings of the same radii: $R = 20 \mu m$ (blue solid-line), $R = 80 \mu m$ (red solid-line) and $R = 150 \mu m$ (black dashed-line).

For filtering with higher finesse, the CROW with different radii of rings is investigated in Fig. 6. The intensity of transmission channel versus wavelength is shown in this figure. By varying the place of the largest ring, three different cases are compared. Due to the symmetry of the structure, the replacement of the first and third ring does not change the frequency spectrum. The interesting result shown in Fig. 6 is that although by varying the ring radii, the resonant wavelengths of the structure are changed and the filtered spectrum undergoes irregular changes, the wavelength of 1546.3 nm for all the selected radii is well filtered in this channel, so, it is the resonant wavelength of structure. In the dashed-line, the FWHM of this resonant wavelength is more than that of solid-line, and dotted-line, so, it is not a good candidate for filtering the mentioned wavelength with higher quality factor.

The best candidate of CROW with the same ring radii and different ring radii, according to the results of Figs. 5 and 6, are compared in Fig. 7. The larger FSR between completely filtered wavelengths (FSR=2.2 nm) is observed by

choosing different ring radii and the finesse is 11 times larger than the case of the same ring radii $R_1 = R_2 = R_3 = 80\,\mu m$. Therefore, the solid-line of Fig. 7 is the best design of CROW among the mentioned radii for filtering the resonant wavelength 1546.3 *nm* with higher finesse. The reported values are according to the best results of the lots of checked radii.
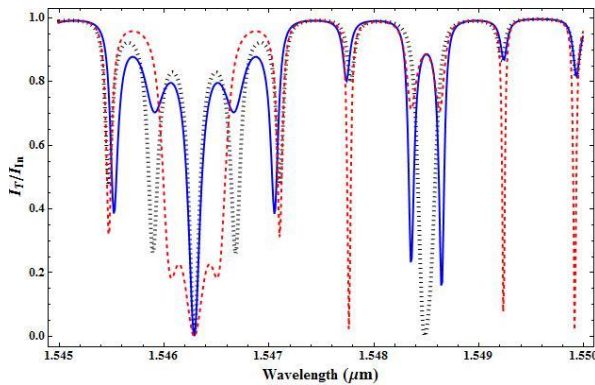

Fig. 6. Transmitted intensity of CROW with the largest ring at the, beginning of structure (blue solid-line, $R_1 = 150\,\mu m$, $R_2 = 50\,\mu m$, and $R_3 = 20\,\mu m$), middle of structure (red dashed-line, $R_1 = 20\,\mu m$, $R_2 = 150\,\mu m$, and $R_3 = 50\,\mu m$) and end of structure (black dotted-line, $R_1 = 50\,\mu m$, $R_2 = 20\,\mu m$, and $R_3 = 150\,\mu m$)
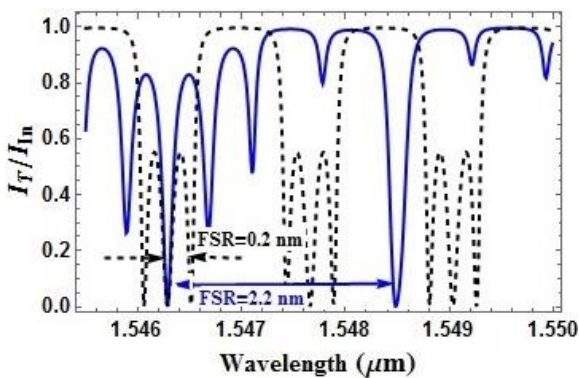

Fig. 7. Comparison the transmission spectrum of CROW with the different ring radii $R_1 = 50\,\mu m$, $R_2 = 20\,\mu m$, and $R_3 = 150\,\mu m$ (solid-line) and the same ring radii $R_1 = R_2 = R_3 = 50\,\mu m$ (dashed -line).

The coupling regions in the structure just change the amplitude of passed or filtered wavelengths and do not change their place in the spectrum. Hence, after choosing the appropriate radii of $R_1 = 50\,\mu m$, $R_2 = 20\,\mu m$, and $R_3 = 150\,\mu m$ to filter the resonant wavelength 1546.3 *nm*, we investigate the effect of different coupling coefficients on the

filter improvement of this signal. In 3D plots of Fig. 8, field intensity variation of transmission channel versus variation of coupling coefficients between rings is shown for different values of coupling coefficient between ring and waveguide.
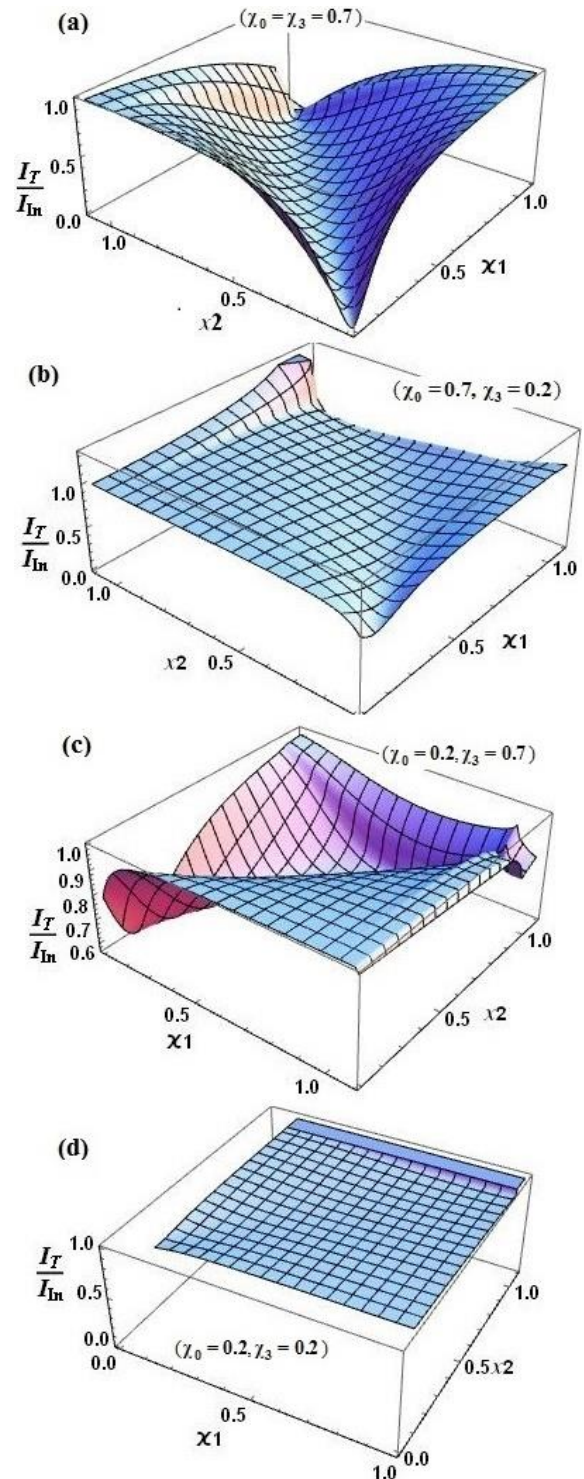

Fig. 8. Variation of field intensity of transmission channel versus coupling coefficient between rings, where the coupling between ring and waveguides are

a) $\left(\chi_0 = \chi_3 = 0.7\right)$, b) $\chi_0 = 0.7$, $\chi_3 = 0.2$, c) $\chi_0 = 0.2$, $\chi_3 = 0.7$, and d) $\chi_0 = 0.2$, $\chi_3 = 0.2$.

In Fig. 8a, where the coupling coefficients between ring and waveguides are $\left(\chi_0 = \chi_3 = 0.7\right)$, the middle curvature of the graph shows that for each pair of the same coupling between rings, the desired wavelength 1546.3 *nm* is well filtered. However, for some other ring and waveguide coupling coefficients, the desired wavelength is never filtered in the transmission channel, as shown in Figs. 8b and 7d and the structure should not be designed as a filter according to these coupling parameters. While the coupling of first ring to the waveguide is large $\left(\chi_0 = 0.7\right)$, the resonant wavelength of structure is well coupled to the rings. However, if the coupling of last ring to the waveguide is small $\left(\chi_3 = 0.2\right)$, it cannot exit from the dropping channel and return to the transmission channel. Thus, it never filters in the transmission channel as shown in Fig. 8b. In Fig. 7c the coupling of waveguide to the first ring is small $\left(\chi_0 = 0.2\right)$ and the coupling of waveguide to the last ring is large $\left(\chi_3 = 0.7\right)$, therefore, the resonant wavelength 1546.3 *nm* is weakly coupled to the rings and it doesn't filter in transmission channel well. Figure 8d shows that for small coupling of first and last ring to the waveguide $\left(\chi_0 = \chi_3 = 0.2\right)$, the resonant wavelength cannot enter to the structure at all to pass through the transmission channel.

Although we have theoretically investigated the structure by Mathematica software as before [53], [54], our results are well consistent with experimental results were explored in [12], [44], [48] for very similar structures to the designed CROW in this study. Also, in [55] the similar CROW was simulated in CST microwave studio and its results do not contradict our data.

IV. CONCLUSION

The combination of ring-resonators called CROW is considered as an optical filter to improve its performance. For this purpose, the effects of variations of the ring radii and the coupling coefficients on the performance characteristics of filtering such as quality factor and finesse are investigated. The transfer matrix method is used to study the behavior of fields in the structure. It is shown that the presence of three coupled rings in the structure comparing with a single ring, increases the filtered wavelengths over the specified range of 1545-1548 *nm* with higher quality factor. Since the resonant wavelengths of structure are influenced by the radius of rings, the transmission channel spectrum for different ring radii is studied. The ring radii which lead to filtering the resonant wavelength with largest finesse value are found. After that, the effect of coupling coefficients on the improvement of filtering the resonant wavelength is discussed. The field intensity variation of transmission channel versus coupling coefficients shows that filtering of the resonant wavelength never occurs for some coupling coefficients. However, for some others, the reverse is true and these coupling parameters would be good candidate for improving system filtering performance. These theoretical results are helpful for experimental design of CROW to filter or pass a specified THz signal with high finesse.

REFERENCES

[1] L.F. Stokes, M. Chodorow, and H.J. Shaw, "All-single-mode fiber resonator," Opt. Lett. Vol. 7, pp. 288-290, 1982.

[2] RM. Shelby, MD. Levenson, and SH. Perlmutter, "Bistability and other effects in a nonlinear fiber-optic ring resonator," J. Opt. Soc. Amer. B Vol. 5, pp. 347-357, 1988.

[3] R. Orta, P. Savi, R. Tascone, and D. Trinchero, "Synthesis of multiple-ring-resonator filters for optical systems," IEEE Photon. Technol. Lett. Vol. 7, pp. 1447-1449, 1995.

[4] S. Malthesha and N. Krishnaswamy, "Improvement in quality factor of double microring resonator for sensing applications,"

J. Nanophoton. Vol. 13, pp. 026014 (1-20), 2019.

[5] A. Noury, X. Le Roux, L. Vivien, and N. Izard, "Carbon nanotube photonics: using microring resonators for tailoring semiconducting carbon nanotubes photoluminescence," J. Nanophoton. Vol.10, pp. 012513 (1-6), 2015.

[6] A.W. Poon, X. Luo, F. Xu, and H. Chen, "Cascaded microresonator-based matrix switch for silicon on-chip optical interconnection," Proc. IEEE 97, pp. 1216-1238, 2009.

[7] B. Troia, V.M. Passaro, A.Z. Khokhar, M. Nedeljkovic, J.S. Penades, and G.Z. Mashanovich, "Design and fabrication of silicon cascade-coupled ring resonators operating in mid infrared," Proc. Fotonica AEIT Italian Conference on Photonics Technologies, pp. 1-4, 2014

[8] G.K. Bharti, J.K. Rakshit, M.P. Singh, and P. Yupapin, "Design of all-optical universal logic gates using mode-conversion in single silicon microring resonator," J. Nanophoton. Vol. 13, pp. 036002 (1-13), 2019.

[9] Y. Chen, J. Feng, Z. Zhou, J. Yu, C.J. Summers, and D.S. Citrin, "Fabrication of silicon microring resonator with smooth sidewalls," J. Micro/Nanolithography, MEMS, and MOEMS, Vol. 8, pp. 043060 (1-5), 2009.

[10] J. Kedia and N. Gupta, "An FDTD analysis of serially coupled double ring resonator for DWDM," Optik, Vol. 126, pp. 5641-5644, 2015.

[11] R. Novitski, B.Z. Steinberg, and J. Scheuer, "Finite-difference time-domain study of modulated and disordered coupled resonator optical waveguide rotation sensors," Opt. Express, Vol. 22, pp. 23153-23163, 2014.

[12] F. Morichetti, C. Ferrari, A. Canciamilla, and A. Melloni, "The first decade of coupled resonator optical waveguides: bringing slow light to applications," Laser Photon. Rev. Vol. 6, pp. 74-96, 2012.

[13] C. Taddei, L. Zhuang, M. Hoekman, A. Leinse, and R. Oldenbeuving, P. van Dijk, and C. Roeloffzen, "Fully reconfigurable coupled ring resonator-based bandpass filter for microwave signal processing," Proc. 9th Asia-Pacific Microwave Photonics Conference (APMP), pp. 44-47, 2014

[14] R.M. Shelby, M.D. Levenson, D.F. Walls, A. Aspect, and G.J. Milburn, "Generation of squeezed states of light with a fiber-optic ring interferometer," Phys. Rev. A, Vol. 33, pp. 4008-4025, 1986.

[15] M.Y. Nada, M.A. Othman, O. Boyraz, and F. Capolino, "Giant resonance and anomalous quality factor scaling in degenerate band edge coupled resonator optical waveguides," J. Lightwave Technol. Vol. 36, pp. 3030-3039, 2018.

[16] C. Taddei, L. Zhuang, C.G. Roeloffzen, M. Hoekman, and K.J. Boller, "High-selectivity on-chip optical bandpass filter with sub-100-MHz flat-top and under-2 shape factor," IEEE Photon. Technol. Lett. Vol. 31, pp. 455-458, 2019.

[17] Z. Bian, B. Liu, and A. Shakouri, "InP-based passive ring-resonator-coupled lasers," IEEE J. Quantum Electron. Vol. 39, pp. 859-865, 2003.

[18] L. Zhou, X. Wang, L. Lu, and J. Chen, "Integrated optical delay lines: a review and perspective," Chin. Opt. Lett. Vol. 16, 101301, 2018.

[19] N.H. Fouad, A.O. Zaki, D.C. Zografopoulos, R. Beccherelli, and M.A. Swillam, "Low power hybrid plasmonic microring-on-disks electro-optical modulators," J. Nanophoton. Vol. 11, pp. 016014 (1-8), 2017.

[20] J.K. Poon, J. Scheuer, S. Mookherjea, G.T. Paloczi, Y. Huang, and A. Yariv, "Matrix analysis of microring coupled-resonator optical waveguides," Opt. Express, Vol. 12, pp. 90-103, 2004.

[21] T.G. Nguyen, K. Yego, G. Ren, A. Boes, and A. Mitchell, "Microwave engineering filter synthesis technique for coupled ridge resonator filters," Opt. Express, Vol. 27 pp. 34370-34381, 2019.

[22] Y. Liu, D. Jiang, W. Cao, T. Yang, L. Xia, and R .Xu, "Microwave tunable split ring resonator bandpass filter using nematic liquid crystal materials," Optik, Vol. 127, pp. 10216-10222, 2016.

[23] S. Xiao, M.H. Khan, H. Shen, and M. Qi, "Multiple-channel silicon micro-resonator based filters for WDM applications," Opt. Express, Vol. 15, pp. 7489-7498, 2007.

[24] Z.Q. Hui, Y. Zhang, M. Yang, S. Wei, M. Zhang, and F. He, "Nonconcentric triple-microring resonator for label-free on-chip sensing with high figure-of-merit," J. Nanophoton. Vol. 11, pp. 036014 (1-14), 2017.

[25] C.K. Madsen and G. Lenz, "Optical all-pass filters for phase response design with applications for dispersion compensation," IEEE Photon. Technol. Lett. Vol. 10, pp. 994-996, 1998.

[26] S. Song, X. Yi, S.X. Chew, L. Li, L. Nguyen, and R. Zheng, "Optical single-sideband modulation based on silicon-on-insulator coupled-resonator optical waveguides," Opt. Eng. Vol. 55, pp. 031114 (1-6), 2015.

[27] S. Javanshir, A. Pourziad, and S. Nikmehr, "Optical temperature sensor with micro ring resonator and graphene to reach high sensitivity," Optik, Vol. 180, pp. 442-446, 2019.

[28] S. Ranjan and S. Mandal, "Performance analysis of quadruple asymmetrical optical micro ring resonator as optical filter," Optik, Vol. 171, pp. 821-832, 2018.

[29] M.R. Almasian and K. Abedi, "Performance improvement of wavelength division multiplexing based on photonic crystal ring resonator," Optik, Vol. 126, pp. 2612-2615, 2015.

[30] M. Humer, R. Guider, F. Hackl, and T. Fromherz, "Polymer-embedded colloidal lead-sulfide nanocrystals integrated to vertically slotted silicon-based ring resonators for telecom applications," J. Nanophoton. Vol. 7, pp. 073076 (1-12), 2013.

[31] L. Gai, J. Li, and Y. Zhao, "Preparation and application of microfiber resonant ring sensors: A review," Optics Laser Technol Vol. 89, pp. 126-136, 2017.

[32] J. Scheuer, "Quantum and thermal noise limits of coupled resonator optical waveguide and resonant waveguide optical rotation sensors," J. Opt. Soc. Amer. B, Vol. 33, pp. 1827-1834, 2016.

[33] D.G. Rabus, *Integrated Ring Resonators: The Compendium*, Springer, pp. 3-34, 2007.

[34] D.H. Geuzebroek and A. Driessen, *Ring-Resonator-Based Wavelength Filters, Wavelength Filters in Fibre Optics*, Berlin: Springer, pp. 341-379, 2006.

[35] Z. Zhou, H. Wu, J. Feng, J. Hou, H. Yi, and X. Wang, "Silicon nanophotonic devices based on resonance enhancement," J. Nanophoton. Vol. 4, pp. 041001 (1-24), 2010.

[36] J.Z. Sun, L. Zhang, and F. Gao, "Switching terahertz waves with graphene-integrated split-ring resonator," Optik, Vol. 127, pp. 8096-8102, 2016.

[37] A. Melloni, "Synthesis of a parallel-coupled ring-resonator filter," Opt, Lett, Vol. 26, pp. 917-919, 2001.

[38] D. Kalantarov, "Tunable low dispersion optical delay line using three coupled micro-resonators," J. Optics, Vol. 19, pp. 115802 (1-13), 2017.

[39] A.M. Prabhu, A. Tsay, Z. Han, V. Van, "Ultracompact SOI microring add–drop filter with wide bandwidth and wide FSR," IEEE Photon. Technol. Lett. Vol. 21, pp. 651-653, 2009.

[40] S.E. El-Zohary, A.A. Azzazi, H. Okamoto, T. Okamoto, M. Haraguchi, and M.A. Swillam, "Resonance-based integrated plasmonic nanosensor for lab-on-chip applications," J. Nanophoton. Vol. 7, pp. 073077 (1-10), 2013.

[41] M.Y. Nada, M.A. Othman, F. Capolino, "Theory of coupled resonator optical waveguides exhibiting high-order exceptional points of degeneracy," Phys. Rev. B, Vol. 96, pp. 184304 (1-15), 2017.

[42] H.L. Liew, *Advanced Silicon Microring Resonator Filter Architectures for Optical Spectral Engineering*, PhD Dissertation, University of Alberta, 2009.

[43] C. Manolatou, M.J. Khan, S. Fan, P.R. Villeneuve, H.A. Haus, and J.D. Joannopoulos, "Coupling of modes analysis of resonant channel add-drop filters," IEEE J. Quantum Electron. Vol. 35, pp. 1322-1331, 1999.

[44] A.M. Prabhu, H.L. Liew, and V. Van, "Experimental determination of coupled-microring filter parameters via pole-zero extraction," Opt. Express, Vol. 16, pp. 14588-14596, 2008.

[45] F. Turri, *Experiments and modelling of vertically coupled Microresonators*, PhD Dissertation, University of Trento, 2017.

[46] D.G. Rabus and C. Sada, *Integrated Ring Resonators*, *Compendium,* Springer, pp. 3-46, 2020.

[47] R.F. Aguinaldo, Silicon photonics with applications to data center networks, PhD Dissertation, University of California, San Diego, 2014.

[48] M. Soltani, S. Yegnanarayanan, Q. Li, and A. Adibi, "Systematic engineering of waveguide-resonator coupling for silicon microring/microdisk/racetrack resonators: theory and experiment," IEEE J. Quantum Electron. Vol. 46, pp. 1158-1169, 2010.

[49] P. Panindre, N.S. Mousavi, B. Paredes, M. Rasras, and S. Kumar, "Coupling and Optical Analysis of a Round-Cornered Square-Shaped Microresonator," Appl. Sci. Vol. 11, pp. 8659, 2021.

[50] S.J. Son, S. Kim, N.E. Yu, and D.K. Ko, "Bus-waveguide-width Dependence of Evanescent Wave Coupling in a Microring Resonator," Current Opt. Photon. Vol. 5, pp. 538-543, 2021.

[51] Q. Li, G. Moille, H. Taheri, A. Adibi, and K. Srinivasan, "Improved coupled-mode theory for high-index-contrast photonic platforms," Phys. Rev. A, Vol. 102, pp. 063506 (1-9), 2020.

[52] W. Bogaerts, P. De Heyn, T. Van Vaerenbergh, K. De Vos, and S, Kumar Selvaraja, T. Claes, P. Dumon, P. Bienstman, D. Van Thourhout, and R. Baets, "Silicon microring resonators," Laser Photon. Rev. Vol. 6, pp. 47-73, 2012.

[53] A.R. Bahrampour, F. Bazouband, and V. Nickfarjam, "Effect of direct coupling of microrings on the gain bandwidth of cascade microring Raman amplifier," Opt. Commun. Vol. 283, pp. 2939-2946, 2010.

[54] A.R. Bahrampour and F. Bazouband, "Gain ripple minimization in the wide-band SCISSOR Raman amplifier," Opt. Commun. Vol. 282, pp. 1648-1653, 2009.

[55] S. Chauhan and R. Letizia, "Photonic crystal-microring resonators for tunable delay lines," arXiv:1811.07828, 2018.

Fateme Bazouband was born in Shiraz in 1981. She studied physics in university and she received her B.Sc in 2004 from Shiraz University, M.Sc. in 2008 from Rafsanjan University and Ph.D in 2013 from Amirkabir University of Technology. She has been studying at the field of optics and photonics for about 12 years and published more than 20 papers. She started teaching in Fasa University just after graduating and she has been a full-time faculty member since 2013.

Amin Rahimpour was born in Fasa in 1979. She studied electronic engineering in university and she received his B.Sc. in 2002 and M.Sc. in 2018 from Islamic Azad University of Fasa. He has been working in Telecommunication Infrastructure Company since 2010.

THIS PAGE IS INTENTIONALLY LEFT BLANK.